Frequency-Based Design of the KDamper Concept for Seismic Isolation of Bridges

Konstantinos A. Kapasakalis, Christos-Habib T. Alamir, Ioannis A. Antoniadis, and Evangelos J. Sapountzakis

Abstract Contemporary seismic isolation systems for bridge structures provide (A) horizontal isolation from the effects of ground motion and (B) an energy dissipation mechanism to reduce displacements. Throughout the years many kinds of seismic isolation mechanisms have been developed, with the concept of introducing negative stiffness being the most promising. In this context, a novel passive vibration isolation and damping concept is introduced, the KDamper. The KDamper is based on the optimal arrangement of stiffness elements, including a negative stiffness element. The main advantage of the KDamper over other similar concepts including negative stiffness elements is that no reduction in the overall stiffness of the system is required. This paper considers the application of a KDamper system to a bridge structure. The system is subjected to artificial accelerograms, designed to be compatible to a rather conservative seismic case corresponding to EC8, ground type C. The mean power spectral density of these accelerograms is used to calculate the effect of the variation of the nominal KDamper frequency to the transfer functions, the response power spectral densities, and the root mean square responses. The KDamper is designed to higher frequencies compared to the isolated system with seismic isolation bearings, exploiting the extraordinary damping properties it offers. A comparison with a seismic isolated structure using Lead Rubber Bearings, designed to greatly increase

K. A. Kapasakalis · C.-H. T. Alamir (✉) · E. J. Sapountzakis
School of Civil Engineering, National Technical University of Athens, Institute of Structural Analysis and Antiseismic Research, Zografou Campus, 157 80 Athens, Greece
e-mail: alamir.christos@gmail.com

K. A. Kapasakalis
e-mail: kostiskapasakalis@hotmail.com

E. J. Sapountzakis
e-mail: cvsapoun@central.ntua.gr

I. A. Antoniadis
Dynamics and Structures Laboratory, Mechanical Engineering Department, National Technical University of Athens, Zografou Campus, 157 80 Athens, Greece
e-mail: antogian@cenral.ntua.gr

E. J. Sapountzakis et al. (eds.), *Proceedings of the 14th International Conference on Vibration Problems*, Lecture Notes in Mechanical Engineering,
https://doi.org/10.1007/978-981-15-8049-9_11

the natural period of the system (2.0 s), confirms that KDamper base seismic absorption designs can provide great reduction to the absolute accelerations reducing at the same time the deck's displacement.

Keywords Seismic isolation · Negative stiffness · KDamper · Damping

1 Introduction

Seismic isolation is probably the only successfully applied alternative for earthquake-resistant design [1], since it achieves the reduction of earthquake-induced lateral loading in the structure, instead of increasing its resistance. Isolation systems separate the heavier superstructure from its foundation, essentially decoupling their response leading to lower seismic loads being imposed in the whole structure. In this context, a variety of isolation devices including elastomeric bearings (with and without lead core) [2], frictional/sliding bearings, roller bearings have been proposed and implemented. The introduction of negative stiffness elements (Negative Stiffness Devices and "Quazi Zero Stiffness" oscillators) has been proposed in the last years. Negative stiffness can be described as a force assisting motion instead of opposing it, contrary to positive stiffness spring. The introduction of negative stiffness elements (or "anti-springs") is not modern, it was initially introduced in the pioneering publication of Molyneaux [3], as well as in the breakthrough developments of Platus [4]. The main idea behind these approaches is the substantial reduction of the isolator stiffness even at almost zero levels leading to the reduction of the natural frequency of the system, as in Carella et al. [5], being thus called "Quazi Zero Stiffness" (QZS) oscillators. A comprehensive review of such concepts can be found in Ibrahim [6]. The negative stiffness response is primarily achieved by complex mechanical designs, combining conventional positive stiffness pre-stressed elastic mechanical elements, such as pre-compressed springs, plates, shells, and post-buckled beams, arranged in appropriate geometrical configurations. Some interesting designs are described in [8, 9]. Among others, QZS oscillators find numerous applications in seismic isolation [7, 10–16].

The increased flexibility of the coupling of the structure with the ground for Base Isolated Structures (BIS) significantly reduces the earthquake-induced forces in the superstructure, which practically behaves as a rigid body. However, because the ground displacement is decoupled from the structure, this results to large relative displacements being concentrated at the isolation level. This fact increases the technological requirements and design complexity of base isolators and has direct effect on the overall performance of the system. Suitable joints for utilities (e.g., waterworks, gas fittings, and electrical conduits) at the isolation level should be provided. An adequate separation distance between adjacent buildings is necessary to prevent collisions or structural pounding [17]. The structure's bearing capacity is reduced for horizontal loads (e.g., winds) for which displacement is expected to be limited during the serviceability ultimate limit state. One of the most important drawbacks is that BIS is in constructability terms and economically prohibitive for retrofitting

existing structures. Increasing the BIS damping ratio ζ_B or, alternatively, introducing supplementary dampers inside the structure to minimize the excessive displacements [18] is not common practice due to its complexity. Besides to the excessive technological demands imposed on the relative devices due to their size and the capacity of the structure to accommodate them, the direct increase of damping can lead to larger interstorey drifts and floor accelerations [19].

Throughout the various active or passive control strategies, the introduction of an additional mass (Tuned Mass Dampers) consists of a common and effective solution for some type of structures. A Tuned Mass Damper (TMD) is a commonly used device consisting of a mass, a spring, and a viscous damper at its most typical form. It is usually attached to a vibrating primary system in order to suppress any undesirable vibrations induced usually by wind and earthquake. The TMD concept was first applied by Frahm [20]. Since Den Hartog [21] first introduced an optimal design method for the TMD for a simple undamped SDoF structure, the TMD implementation in skyscrapers is among the most interesting ones [22–24]. A characteristic example of its application on skyscrapers can be found in one of the tallest buildings in the world, Taipei 101 Tower (101 stories, 504 m) in Taiwan [25]. Recent studies also include the application of TMDs for vibration mitigation in seismic or other forms of excitation like wind induced vibrations of bridge structures [26]. The natural frequency of the TMD is tuned in resonance with the fundamental mode of the primary structure. Thus, a large amount of the structural vibrating energy is transferred to the TMD and then dissipated by damping. Even though TMDs are known for their effectiveness and their reliability, their usage encounters significant disadvantages. Environmental conditions and other external parameters may alter the TMD properties, disturbing its tuning. Consequently, the device's performance can be significantly reduced [27]. Another drawback of the TMD is that a substantial oscillating mass is required in order to achieve effective vibration reduction complicating its construction and installation procedure.

The novel KDamper concept introduced by Antoniadis et al. [28] integrates the effective design aspects of both Negative Stiffness Elements and Tuned Mass Dampers. The device under consideration makes use of a negative stiffness element, which enhances the device's damping properties, avoiding the deficiencies of TMDs or QZS oscillators. The KDamper is designed to maintain the same overall (static) stiffness as the original reference oscillator. However, it differs from both the original SDoF oscillator and existing negative stiffness oscillators, due to the effective combination of the individual stiffness elements and the reallocation of the damping. Usually negative stiffness elements exhibit an unstable behavior, the device under consideration is set up in a way to be statically and dynamically stable. The incorporation of an additional mass mitigates the oscillation effects, acting as an energy dissipation mechanism similar to the mass of TMDs. In contrast with TMDs the KDamper overcomes the sensitivity problems of tuning since this is mainly controlled by the negative stiffness element's parameters. Optimization of the device's controlling parameters leads the system to exhibit exceptional damping characteristics. The optimal selection for the KDamper parameters can be based on the minmax ($H\infty$) approach, initially introduced by Den Hartog [21]. Relevant methods are

described in Antoniadis et al. [28] for a Force Excitation/Displacement Response Transfer Function and in [29–32] for a base acceleration excitation/relative structure displacement response transfer function. A different design approach, implementing an optimization algorithm, is presented in Syrimi et al. [33].

In this paper, the feasibility of the KDamper as an alternative or supplement to conventional seismic isolation of bridge structures is examined. The aim is the optimization of the KDamper parameters with respect to the provisions of the design spectra of the various seismic codes and to evaluate the advantages of its use in the response of the system. The concept of KDamper is presented in Sect. 2, along with a preliminary conceptual presentation on its fundamental concept and an explanation of how this device could potentially overcome the drawbacks of the typical vibration absorbers: the Quazi Zero Stiffness Oscillator and the Tuned Mass Damper. The optimal selection approach of the KDamper parameters is also introduced in Sect. 2, which follows the same steps of Den Hartog [21]. Finally, Sect. 2 provides an overview of the basic KDamper properties. The KDamper always indicates better isolation properties than a TMD damper with the same additional mass. Instead of increasing the additional mass, the vibration isolation capability of the KDamper can be increased by increasing the value of the negative stiffness element. Section 3 provides an overview of the so-called "Design Response Spectra". A database of artificial accelerograms is produced, calibrated to be compatible with a rather conservative seismic case corresponding to EC8, ground type C. The mean acceleration response spectrum is calculated, matching accurately the EC8 response spectra. The least square fitting of the mean power spectral densities, of the total number of accelerograms in the database, is calculated and used as the ground motion excitation acceleration PSD. The response power spectral densities are formed and the root mean square responses are derived, as an indicator of the actual energy content of the response. Section 4 presents a spectral driven optimization of the KDamper natural frequency for seismic isolation of a typical bridge structure. The transfer functions, response power spectral densities, and root mean square responses are formed and confirmed in the time domain. Two alternative options for the implementation of the KDamper are considered. Initially, the nominal KDamper frequency is selected equal to the frequency of a typical base isolated structure (0.4 Hz), resulting in a substantial reduction of the absolute structure acceleration. Alternatively, another promising option is examined, which foresees the implementation of the KDamper, as a stiffer base absorption system, with a nominal frequency much higher than that of the initial isolation system. The selection of a higher value for the nominal frequency dramatically reduces the relative deck displacement combined with an acceptable dynamic response in terms of absolute acceleration. Therefore, the KDamper can be implemented as a "stiff seismic absorption base", resulting to relative deck displacements in the order of few centimeters and consequently to overcome the drawbacks of conventional base isolation systems and dictate alternative seismic protection technologies.

2 Overview of the KDamper Concept

Figure 1 shows three concepts of seismic isolation systems and their basic characteristics. Each one is designed in a way to minimize the response $x(t)$ of an undamped SDoF system of mass m and static stiffness k of to a base excitation of $x_G(t)$. The Negative Stiffness isolator, in Fig. 1a achieves the total stiffness of the system to be: $k_{QZS} = k + k_N \leq k$ this is done by adding a negative stiffness element k_N parallel to the element stiffness k of the original structure. Yet this results in the reduction of the static bearing capacity of the system, limiting its application for horizontal isolation due to wind or service loads inducing considerable deformations, the same applies for vertical vibration isolation. Figure 1c introduces the basic concept of the KDamper which also implements a negative stiffness element k_N. However, contrary to the QZS isolator, the fundamental design parameter of the KDamper is that the overall static stiffness of the isolated system remains the same as the original one, Eq. (1):

$$k_R + \frac{k_P k_N}{k_P + k_N} = k \tag{1}$$

This is how the KDamper avoids the main drawback of the QZS isolator. Compared to the TMD (Fig. 1b), the KDamper incorporates an additional negative stiffness element k_N, which connects the additional mass to the base. Consequently, the equation of motion of the KDamper becomes

$$m\ddot{u}_S + k_R u_S + m_D \ddot{u}_D + k_N u_D = -(m + m_D)a_G \tag{2a}$$

$$m_D \ddot{u}_D - c_D(\dot{u}_S - \dot{u}_D) - k_P(u_S - u_D) + k_N u_D = -m_D a_G \tag{2b}$$

Assuming a harmonic excitation in the form of $a_G(t) = A_G e^{j\omega t}$ and a steady state response of $u_S(t) = \tilde{U}_S \exp(j\omega t)$ and $u_D(t) = \tilde{U}_D \exp(j\omega t)$, where $\tilde{U}_S$, $\tilde{U}_D$ denote

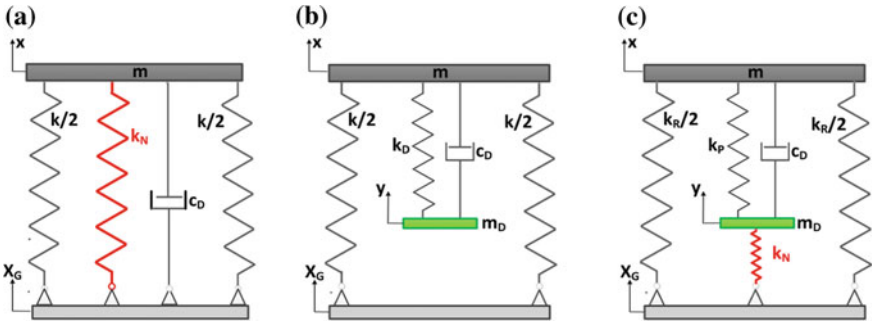

Fig. 1 Schematic presentation of the considered vibration absorption concepts **a** Quasi-Zero Stiffness (QZS) oscillator, **b** Tuned Mass Damper (TMD), and **c** KDamper

complex quantities, the equations of motion (2a, 2b) of the KDamper become

$$-\omega^2 m\tilde{U}_S + k_R\tilde{U}_S - \omega^2 m\tilde{U}_D + k_N\tilde{U}_D = -(m+m_D)A_G \tag{3a}$$

$$-\omega^2 m_D\tilde{U}_D - j\omega c_D(\tilde{U}_S - \tilde{U}_D) - k_P(\tilde{U}_S - \tilde{U}_D) + k_N\tilde{U}_D = -m_D A_G \tag{3b}$$

Focusing on Eq. (3a, 3b) it can be understood that the amplitude F_{MD} of the inertia force of the additional mass and the amplitude F_N of the negative stiffness force:

$$F_{MD} = -\omega^2 m_D\left|\tilde{U}_D\right|;\ F_N = k_N\left|\tilde{U}_D\right| \le 0 \tag{4}$$

are exactly in phase, this is the result of the negative value of k_N. Thus, the KDamper can be considered as an indirect approach to increase the inertia effect of the additional mass m_D without, however, increasing directly the mass m_D itself. Additionally, it is worth mentioning that the value of F_{MD} is frequency dependent, while the value of F_N is constant in the entire frequency range, a crucial characteristic for low-frequency vibration isolation.

2.1 Selection of the KDamper Parameters for Optimal Acceleration Response Under Base Excitation

Based on Eqs. (3a, 3b) some important Transfer Functions of the KDamper can be produced:

$$\tilde{H}_{US} = \frac{\tilde{U}_S}{A_G} = -\frac{\tilde{N}_{US}}{\tilde{D}};\ \tilde{H}_{UD} = \frac{\tilde{U}_D}{A_G} = \frac{(j\omega c_D + k_P)H_{US} - m_D}{\left(-\omega^2 m_D + j\omega c_D + k_p + k_N\right)} = \frac{\tilde{N}_{UD}}{\tilde{D}};$$
$$\tilde{H}_{AS} = \frac{\tilde{A}_S}{A_G} = 1 - \omega^2\tilde{H}_{US} = \frac{\tilde{N}_{AS}}{\tilde{D}}, \tag{5}$$

where

$$\tilde{N}_{US} = -\omega^2 m m_D + j\omega c_D(m+m_D) + m(k_P+k_N) + m_D k_P \tag{6a}$$

$$\tilde{N}_{UD} = -\omega^2 m m_D + j\omega c_D(m+m_D) + mk_P + m_D(k_R+k_P) \tag{6b}$$

$$\tilde{N}_{AS} = -\omega^2 m_D k_R + j\omega c_D(k_R+k_N) + k(k_P+k_N) \tag{6c}$$

$$\begin{aligned}\tilde{D} =& \omega^4 m m_D - j\omega^3(m+m_D)c_D - \omega^2[m(k_P+k_R) + m_D(k_P+k_R)] \\ &+ j\omega c_D(k_R+k_N) + k(k_P+k_N),\end{aligned} \tag{6d}$$

where k is the total static stiffness of the system, as described in Eq. (1). Optimization of the KDamper parameters can be based on the classical minmax ($H\infty$) approach, first introduced by Den Hartog [21]. This process is presented in Antoniadis et al. [28] for a Force Excitation/Displacement Response Transfer Function and in [29–32] for a base acceleration excitation/relative structure displacement response transfer function. A different method for parameter definition, making use of an optimization algorithm, is described in Syrimi et al. [33].

Nonetheless, the optimization results have significant discrepancies, which arise due to the different transfer function to be selected for optimization. This is presented in [28], where optimization of the H_{US} transfer function gives non-optimal designs of H_{AS} which presents large lobes in the main seismic excitation area. Such behavior is to be expected, among others based on the analysis of Sect. 1 about the inherent conflict between relative displacement and absolute acceleration simultaneous minimization. Therefore, optimization of the absolute acceleration transfer function H_{AS} is selected in this paper. Equation (5) are brought to a non-dimensional form with respect to the natural frequency of the system ω_0 (Eq. 7b), using the following parameters:

$$\kappa = -k_N/(k_P + k_N);\ \mu = m_D/m \tag{7a}$$

$$\rho = \omega_D/\omega_0;\ q = \omega/\omega_0;\ \omega_0 = \sqrt{k/m};\ \omega_D = \sqrt{k_D/m_D};\ \zeta_D = c_D/2\sqrt{k_D m_D}. \tag{7b}$$

As a result, Eq. (2.5) can be written in the form:

$$\tilde{H}_{AS} = -\frac{A + (j2\zeta_D)B}{C + (j2\zeta_D)D};\ H_{AS} = \frac{\left|\tilde{A}_S\right|}{A_G} = \frac{A_S}{A_G} = \sqrt{\frac{A^2 + (2\zeta_D)^2 B^2}{C^2 + (2\zeta_D)^2 D^2}}, \tag{8}$$

where $A = -q^2[1 + \kappa(1 + \kappa)\mu\rho^2] + \rho^2$, $B = \rho q(1 + \kappa^2\mu\rho^2)$, $C = q^4 - q^2[1 + \rho^2 + (1 + \kappa)^2\mu\rho^2] + \rho^2$ and $D = \rho q[(1 + \kappa^2\mu\rho^2) - q^2(1 + \mu)]$.

The transfer function for the TMD can be derived from Eq. (8) if $\kappa = 0$. The Transfer Function in Eq. (2.8) has only four parameters: κ, μ, ρ, and ζ_D. Initially, the parameters μ and κ are defined from the original system under consideration and the structural capacity available for an additional mass. Next, the optimal value of ρ is dependent from κ, μ (Eq. A.10), following the minmax approach described in Appendix A. Finally, for the selection of ζ_D, numerous methods are possible, whose presentation is beyond the scope of this paper. A direct approach is to calculate ζ_D so that it minimizes the peak of the Transfer Function $H_{AS}(q,\zeta_D)$. Figure 2 presents the variation of $H_{AS}(q,\zeta_D)$ for various values of ζ_D. As it can be observed, for the optimum value of $\zeta_{Dopt} = \zeta_{min}$, both peaks of the Transfer Function $H_{AS}(q,\zeta_D)$ are equal and minimum. Once the values of the mass μ and the total stiffness κ are known, the values of the elements of the KDamper thus finally result as

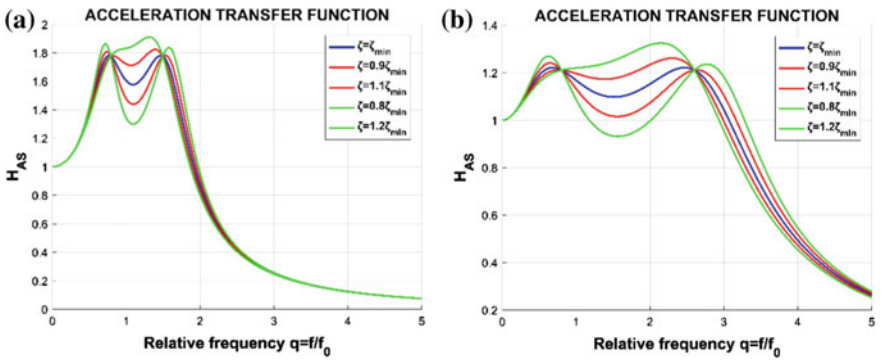

Fig. 2 Dependence of transfer function H_{UAS} on the damping ratio ζ_D **a** $\mu = 0.05$, $\kappa = 2.56$ **b** $\mu = 0.05$, $\kappa = 3.41$

$$k_N/k = \kappa_N = -\kappa\mu\rho^2;\ k_P/k = \kappa_P = (1+\kappa)\mu\rho^2;\ k_R/k = \kappa_S = 1+\kappa(1+\kappa)\mu\rho^2 \tag{9a}$$

$$m_D = \mu m;\ c_D = 2\zeta_D\sqrt{(k_P + k_N)m_D}. \tag{9b}$$

2.2 Basic Properties of the KDamper

A first fundamental property of KDAMPER is that the addition of a negative stiffness spring reduces the magnitude of the transfer function, as compared to that of a TMD with the same value of μ, as observed in Fig. 3. Moreover, increasing the value of κ reduces the maximum part of the transfer function H_{AS}, which becomes flatter.

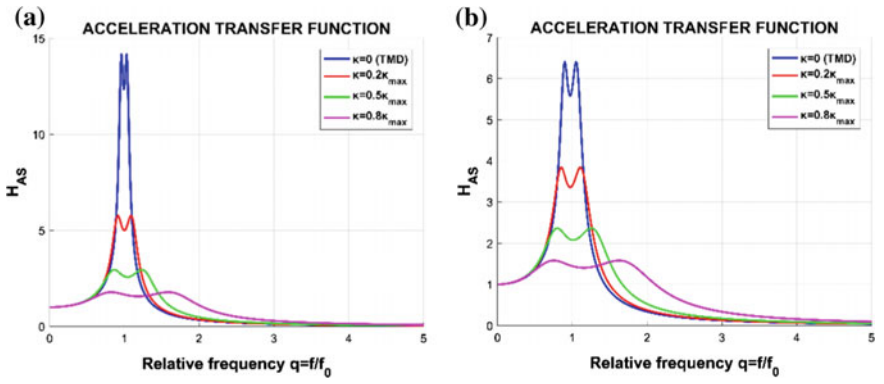

Fig. 3 Effect of the stiffness ratio κ on the transfer function H_{AS} of the KDamper for **a** $\mu = 0.01$ and **b** $\mu = 0.05$

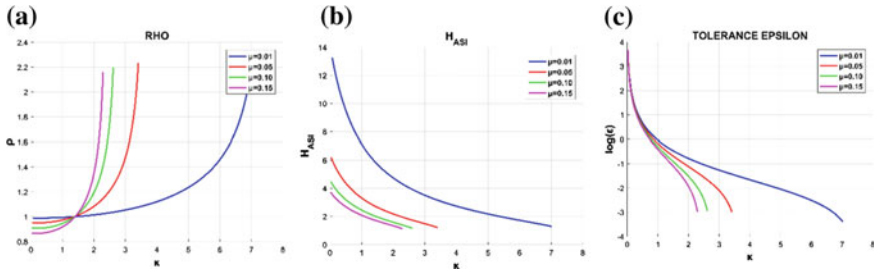

Fig. 4 Effect of the variation of the κ and μ KDamper parameters on **a** the value of $\rho = \omega_D/\omega_0$, **b** the value H_{ASI} of the transfer function at the invariant points q_L, q_R, and **c** the static stability margin ε

Following that, the KDamper is more resistant to detuning, than the TMD. The increase in the value of κ is upper limited by a value of κ_{max}. As observed in Fig. 4a, when κ reaches κ_{max} the frequency ratio ρ tends to infinity. At the same time, (Fig. 4b) transfer function H_{ASI} (Equation A2) of the KDamper at the points q_L and q_R tends to zero.

However, increasing κ has a number of implications in the design of the KDamper. From a dynamics point of view, the transfer function tends to present a more broad-band behavior, as for example observed in Figs. 2 and 3. Moreover, the displacement of the "internal" degree of freedom u_D tends to increase. In view of Eq. (5):

$$\frac{\tilde{H}_{UD}}{\tilde{H}_{US}} = \frac{-\omega^2 m m_D + j\omega c_D(m + m_D) + m k_P + m_D(k_R + k_P)}{-\omega^2 m m_D + j\omega c_D(m + m_D) + m(k_P + k_N) + m_D k_P} \tag{10a}$$

or in a non-dimensional form:

$$\frac{\tilde{H}_{UD}}{\tilde{H}_{US}} = \frac{-q^2 + 2j\rho q\zeta_D(1+\mu) + 1 + (1+\kappa)(1 + (1+\mu+\kappa\mu)\rho^2}{-q^2 + 2j\rho q\zeta_D(1+\mu) + (1+\mu+\kappa\mu)\rho^2}. \tag{10b}$$

In the specific case of $\omega = 0$, $m_D = 0$ Eq. (10b) becomes

$$\frac{\tilde{H}_{UD}}{\tilde{H}_{US}} = 1 + \kappa \tag{11}$$

As a qualitative remark from Fig. 5, increasing κ tends to increase u_D while increasing μ tends to decrease u_D.

From a technological point of view, increasing κ results in high stiffness values of the internal KDamper elastic elements, as presented in Fig. 6. More importantly, increasing the absolute value of the stiffness k_N may put the static stability of the structure at risk. Despite that theoretically the value of k_N is selected based on Eq. (5) to ensure the static stability of the system. The value of k_N can have variations in practice due to several reasons such as temperature variations, manufacturing

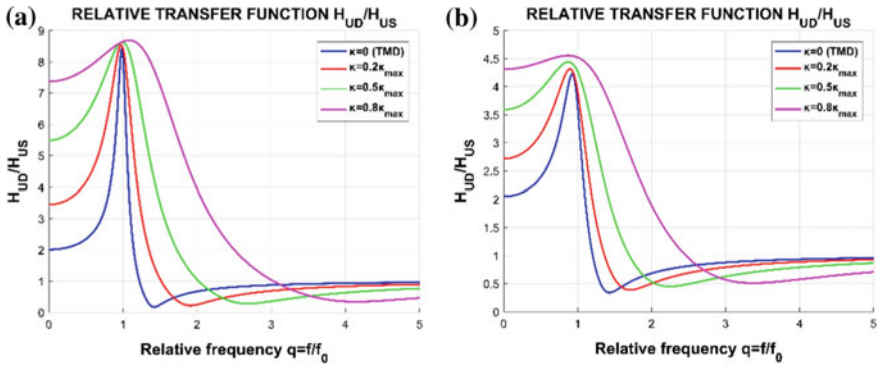

Fig. 5 Effect of the stiffness ratio κ on the ratio of Transfer Functions H_{UD}/H_{US} of the KDamper for **a** $\mu = 0.01$ and **b** $\mu = 0.05$

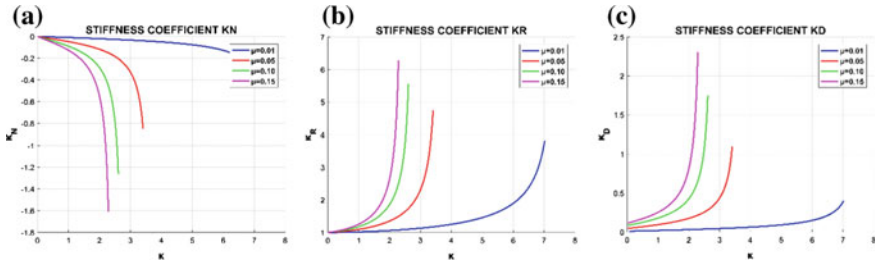

Fig. 6 Effect of increasing κ on the values of stiffness elements of the KDamper. **a** κ_N, **b** κ_P, and **c** κ_R

tolerances, or non-linear behavior, because almost all negative stiffness designs result from unstable non-linear systems. Based on that, an increase of the absolute value of k_N by a factor ε may lead to a new value of k_{NL} where the structure becomes unstable:

$$k_R + \frac{k_P k_{NL}}{k_P + k_{NL}} = 0 \Leftrightarrow k_{NL} = -\frac{k_R k_P}{k_R + k_P} = (1 + \varepsilon) k_N \tag{12}$$

Substitution of Eqs. (9a) into (12) leads to the following estimate for the static stability margin $\varepsilon = 1/(\kappa[(1 + (1 + \kappa)^2 \mu \rho^2])$. Figure 4c presents the variation of ε over κ and μ. As it can be observed from the aforementioned expression of the static stability margin ε and Fig. 4c, the increase of the negative stiffness of the system is upper bounded by the static stability limit of the structure, where ε tends to zero.

3 Design Response Spectrum, Compatible Ground Motion Spectra, Response Power Spectral Densities, and Mean Square Responses

Seismic design codes specify that the structure relative displacement or acceleration is within specified limits for a specific fundamental structure period and damping ratio. These limits strongly depend on the specific ground conditions and expected seismic intensity as well as on the fundamental structural period, thus resulting in the so-called "Design Response Spectra". A typical form of these spectra is depicted in Fig. 7.

However, the direct application of this approach to the selection of the KDamper parameters is not possible, since the application of the KDamper as a base absorption layer leads to an MDoF system with multiple frequencies. For this reason, time history analysis is required for the optimal design of the KDamper. Strong earthquake time histories are generated from one of three fundamental types of accelerograms: synthetic records obtained from seismological models, actual recordings of earthquakes (not all soil combinations are covered, not smoothed spectra) and artificial records, fitted to match code design spectrums, which is the most proper method.

The creation of artificial accelerograms compatible with a selected design spectrum is a very complicated task and consists of a field of research on its own, it is well presented in [34, 35]. The complexity is the result of the earthquakes transient nature, in addition to the fact that the design spectra represent values in the time domain which is demanding to match with spectral values in the frequency domain. As a result, the approach followed in this paper is based on first generating a sample of artificial accelerograms whose response spectra is closely compatible with the design response spectrum (EC8). Artificial spectrum-compatible accelerograms can be generated using SeismoArtif Software [36]. SeismoArtif computes a power spectral density function from a specified smooth response spectrum, in this

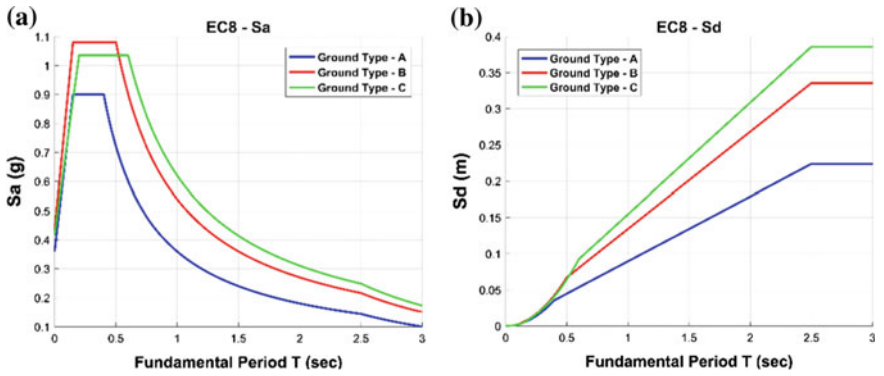

Fig. 7 EC8 Design response spectra: **a** Spectral acceleration and **b** Spectral displacement

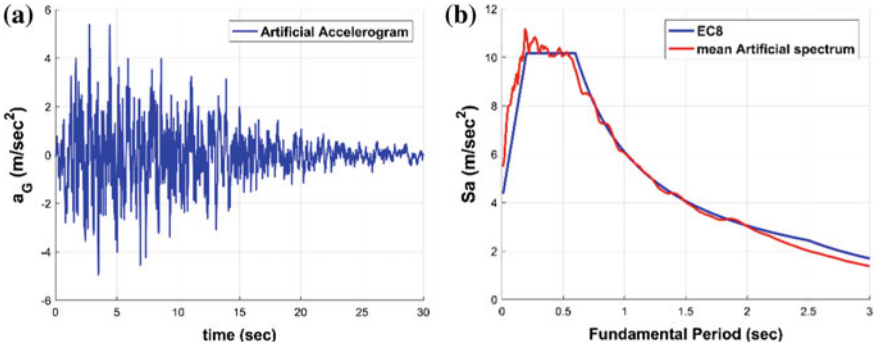

Fig. 8 **a** Artificial Accelerogram and **b** mean Artificial Acceleration response spectra of 30 Artificial Accelerograms compared to the EC8 acceleration design response spectra

case, EC8-Ground type C, and uses this function to derive the amplitudes of sinusoidal signals which have random phase angles. The sinusoidal motions are then summed, and an iterative procedure can be invoked to improve the match with the target response spectra. The power spectral density function is then adjusted by the square of the ordinate ratio and a new motion is generated. In order to get other characteristics of artificial spectrum-compatible record, such as duration, it is necessary to obtain supplementary information about the expected earthquake motion, apart from the response spectrum (envelope shapes). The Artificial Accelerograms used in this paper are designed to match a rather conservative but realistic case: the EC8 response spectrum for a certain ground type, in this case ground type C was considered, for spectral acceleration 0.36 g, spectrum type I and importance class II. In Fig. 8a, an Artificial Accelerogram is presented, applying the calculation method Artificial Accelerogram Generation and Adjustment with an envelope shape proposed by Saragoni and Hart [37].

Next, the mean acceleration response spectrum is calculated and compared to the EC8 design response spectrum. As observed in Fig. 8b, the mean acceleration response spectrum, for 30 Artificial Accelerograms, is matched very accurately with the EC8 response spectrum, with characteristics: spectral acceleration 0.36 g, ground type C, spectrum type I, and importance class II. More specifically, the percentage deviation is under 10% in the range of periods from 0.2 to 2 s, which is of actual concern.

Next, the mean power spectral density S_{AM} of the accelerograms is calculated as $\mathrm{S_{AM}} = (\sum Sai)/Na$, where S_{ai} is the PSD of each acceleration record and Na is the number of accelerograms in the database. The mean power spectral density S_{AM} of the $Na = 30$ accelerations in the selected database is presented in Fig. 9, along with the least square fitting which will be subsequently used as the ground motion excitation acceleration PSD S_A. Having defined the ground motion excitation acceleration PSD S_A, the response power spectral densities, S_{US}, $S_{UD,}$ and S_{AS} of the system main responses can be derived:

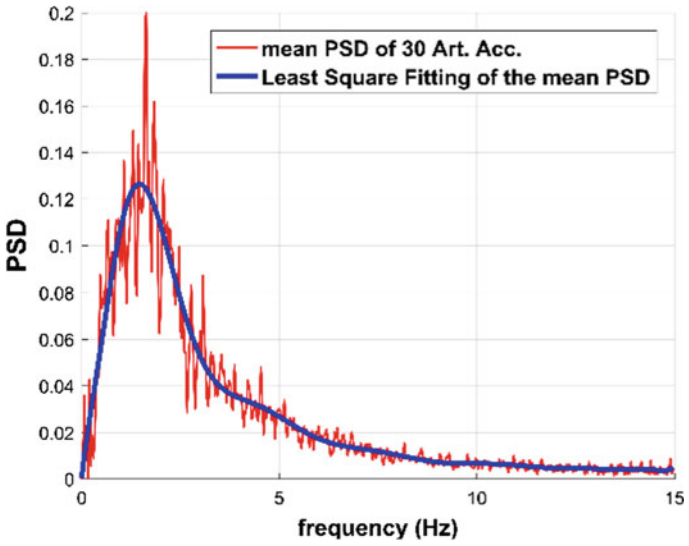

Fig. 9 Mean Power Spectral Density of the 30 Artificial Accelerograms S_{AM} in the selected database with the least square fitting S_A

$$S_{US}(\omega) = H_{US}^2(\omega) S_A(\omega);\ \ S_{UD}(\omega) = H_{UD}^2(\omega) S_A(\omega);\ \ S_{AS}(\omega) = H_{AS}^2(\omega) S_A(\omega) \tag{13}$$

where H_{US}, H_{UB}, $H_{UD,}$ and H_{AS} are the transfer functions of the main system responses. It should be emphasized that the design response spectra of the seismic design codes (e.g., those in Fig. 7), are entirely different than the response power spectral densities of Eq. (13). The root mean square value of the responses is defined next as the root of the area under the power spectral density curve, as an indication of the actual energy content of the response:

$$R_{US} = \left[\int_{-\infty}^{+\infty} S_{US}(\omega) d\omega\right]^{0.5};\ \ R_{UD} = \left[\int_{-\infty}^{+\infty} S_{UD}(\omega) d\omega\right]^{0.5};$$
$$R_{AS} = \left[\int_{-\infty}^{+\infty} S_{AS}(\omega) d\omega\right]^{0.5}. \tag{14}$$

4 Spectral Driven Optimization of the KDamper Natural Frequency

4.1 Test Case Considered

A typical single-pier concrete bridge of mass $m_S = 729.3tn$ with two spans of *25 m* each is considered. The deck is 9.50 m wide. A schematic representation of the bridge is given in Fig. 10. As an initial approach, the pier is considered stiff enough to be neglected. A possible implementation of the KDamper is presented in Fig. 1c. The equations of motion of the new system are Eqs. 2.2a and 2.2b. The new system's parameters μ, κ, and ρ are selected according to the procedure described previously.

In order to observe the effect of the natural frequency of the KDAB system to (1) the transfer functions, (2) the response power spectral densities, (3) the root mean square responses, and (4) the mean peak amplitude responses, of the main system parameters, two characteristic cases are considered. The first case is to match the natural frequency of the KDAB with the BIS system's frequency (low frequency of *0.4* Hz). This case will be referred to hereafter as KDAB-L (KDamper Absorption Base—Low frequency). In the second case, a stiffer base is considered, with a natural frequency of *1* Hz, in order to examine if the large base's displacements, that are

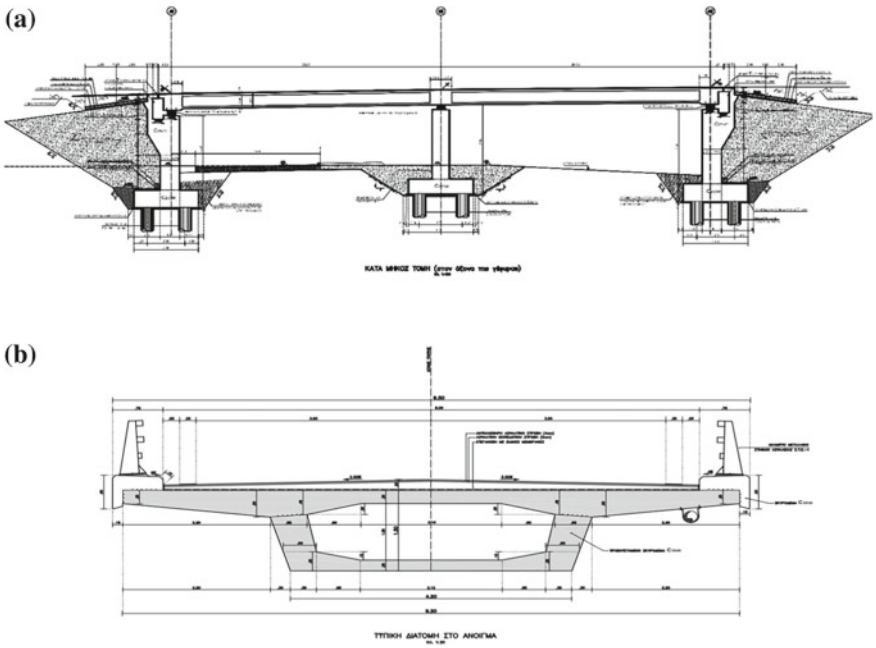

Fig. 10 Schematic representation of the bridge considered. **a** Longitudinal section, **b** Transverse section

Table 1 Parameters of the KDAB-L and KDAB-H systems (L–low frequency, H–high frequency)

System	μ (%)	κ	ζ_D	ε (%)	f_0 (Hz)
KDAB-L	5	3.41	0.622	5	0.4
KDAB-H	5	3.41	0.622	5	1

required in the classical seismic isolation concept, can be avoided. This case will be referred to hereafter as KDAB-H (KDamper Absorption Base—High frequency). The parameters of the KDAB-L and KDAB-H are presented in Table 1.

4.2 *Effect of the Isolation Frequency on the Displacement and Acceleration Transfer Functions*

Figure 11 presents the transfer functions of the main system responses. The Base Isolated System (BIS) system has an $f_B = 0.4$ Hz and a damping ratio of *20%* and the KDamper Absorption Base systems have a natural base frequency of *0.4* Hz (KDAB-L) and *1.0* Hz (KDAB-H), respectively

The effect of the KDamper, implemented to the bridge structure, leads to a significant reduction to the BIS maximum value of the transfer function H_{AS} (absolute acceleration), which becomes now a low pass filter (Fig. 11a), while at the same time retains a significant frequency content. The transfer function of the deck's relative displacement H_{US} is dramatically improved in all frequency range with the implementation of the KDAB system. Increasing the natural frequency of the KDAB from 0.4 Hz (KDAB-L) to 1.0 Hz (KDAB-H), the base's relative displacement H_{US}, as well as the KDamper's relative displacement H_{UD}, are dramatically improved.

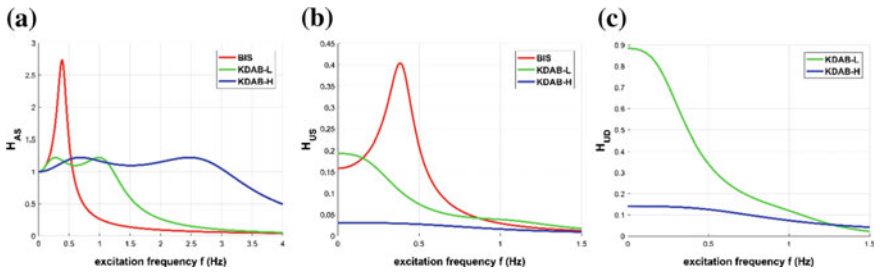

Fig. 11 Transfer Functions of the main system responses **a** structure's absolute acceleration H_{AS}, **b** structure's relative displacement $H_{US,}$ and **c** KDamper relative displacement H_{UD} for all the considered systems: BIS, KDAB-L, and KDAB-H

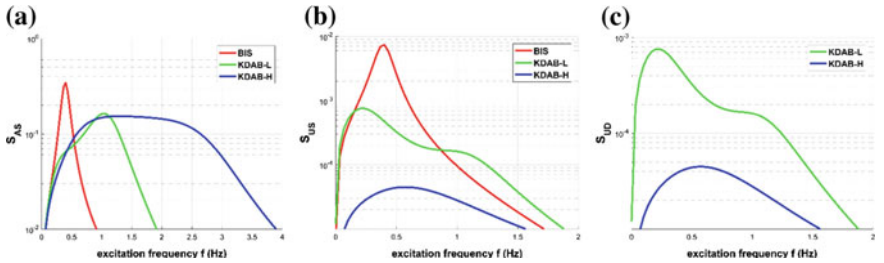

Fig. 12 Response Spectrum Power Densities of the main system responses **a** structure's absolute acceleration S_{AS}, **b** structure's relative displacement S_{US}, and **c** KDamper relative displacement S_{UD} for all the considered systems: BIS, KDAB-L, and KDAB-H

4.3 Effect of the Isolation Frequency on the Response Power Spectral Densities

Based on the design spectrum-compatible ground motion acceleration spectrum S_A of Fig. 8a, the response power spectral densities of all three alternative systems of Fig. 11 are obtained and depicted in Fig. 12. Figure 12a presents the response power spectra density S_{AS}. It is observed that the considered control systems (KDAB-L, and KDAB-H) manage to reduce the BIS's maximum values of the S_{AS}. The frequency content of these response power spectral densities is increasing in the following order: BIS, KDAB-L, and KDAB-H.

KDamper absorption base concepts present a dramatic improvement in the response power spectral density S_{US}, compared with the BIS system. More specifically, although the KDAB-L system has the same base natural frequency (0.4 Hz), it manages to reduce the maximum value of the S_{UB} over one order of magnitude, and KDAB-H which represents the same concept with the KDAB-L, but with a stiffer base (higher nominal frequency), reduces the maximum value of S_{UB} more than two orders of magnitude (Fig. 12b). Finally, by making a stiffer base (KDAB-H), the KDamper's relative displacement power spectral density is reduced more than one order of magnitude (Fig. 12c).

4.4 Effect of the Isolation Frequency on the Root Mean Square Responses and Mean Peak Amplitude Responses

Figure 13 presents the structure's absolute acceleration, the deck's relative displacement, and the KDamper's relative displacement mean square responses ratio:

$$r_{US} = \frac{R_{US}}{R_{US}(ref)} \; r_{AS} = \frac{R_{AS}}{R_{AS}(ref)} \; r_{UD} = \frac{R_{UD}}{R_{US}(ref)}, \tag{15}$$

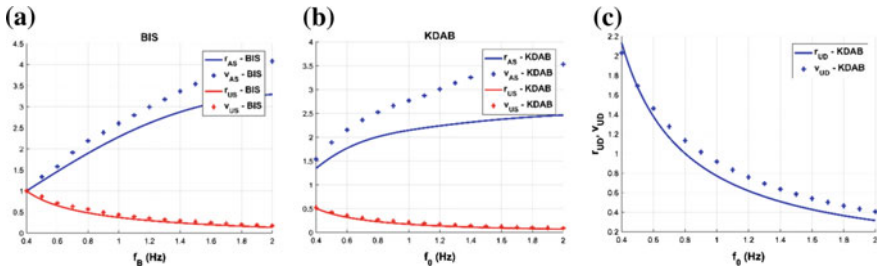

Fig. 13 Root mean square responses ratio (*solid lines*) and verification with mean of the maximum dynamic responses ratio (*dotted lines*), of 30 Artificial Accelerograms, of the BIS system with a damping ratio of *20%* and the KDAB system with parameters: $\mu = 0.05$, $\kappa = 3.41$ and $\zeta_D = 0.622$ **a** BIS's dynamic responses, **b** KDAB's system dynamic responses, and **c** KDamper's relative displacement, over the base's natural frequency f_B, f_0

where $R_{US}(ref)$ and $R_{AS}(ref)$ pertain to the initial BIS system with a natural frequency of *0.4* Hz and a damping ratio of *20%*. The results concern the BIS system with a damping ratio of $\zeta_B = 20\%$ and a continuous variation of the its natural frequency in the range $f_B = [0, 4–2.0]$ Hz, and the KDAB system with parameters $\mu = 5\%$, $\kappa = 3.41$, $\zeta_D = 0.622$ and a continuous variation of the base's natural frequency in the range $f_0 = [0, 4–2.0]$ Hz. The inherent conflict between the requirement for the simultaneous minimization of the structure's absolute acceleration and relative displacement is observed. Figure 13 shows that the deck's absolute acceleration reduction of the BIS and KDAB systems, are at similar levels, while the base becomes less stiff (decreasing the base's natural frequency). The implementation of a KDamper as an absorption base reduces the base's relative displacement more than 50% in all the considered base's frequency range (f_B, f_0).

Next, the equations of motion of the BIS and KDAB, respectively, are solved for all the 30 accelerograms of the database.in the time domain, using the Newmark-β method with linear acceleration. The mean of the ratio of the maximum responses of the dynamic response is defined as

$$v_{US} = \frac{V_{US}}{V_{US}(ref)} \; v_{AS} = \frac{V_{AS}}{V_{AS}(ref)} \; v_{UD} = \frac{V_{UD}}{V_{US}(ref)}, \tag{16}$$

where V_{US}, V_{AS}, V_{UD} are the mean of the maximum systems dynamic responses and $V_{US}(ref)$, $V_{AS}(ref)$ pertain to the initial BIS system with a natural frequency of *0.4* Hz and a damping ratio of *20%*. The results are also presented in Fig. 13 and clearly confirm that a spectral driven design of a control system is accurate, and more specifically a spectral driven optimization of the KDAB base's natural frequency is possible.

Table 2 List of structure's absolute acceleration, considering max values of the dynamic responses, and the % reduction compared with the mean PGA of the 30 Artificial Accelerograms

	BIS	KDAB-L	KDAB-H
max(As) (*m/sec^2*)	1.323	2,064	3,692
(%)	74,52	60,24	28,87

Table 3 List of structure's relative displacement, considering max values of the dynamic responses, and the % reduction compared with the base isolation concept, BIS

	BIS	KDAB-L	KDAB-H
max(Us) (*m*)	0.183	0.090	0.038
(%)	–	50.81	79.23

4.5 Numerical Results—Time Histories

The dynamic responses, considering the max values of the dynamic responses of all 30 Artificial Accelerograms in the database, of the initial BIS system and the controlled system with the two considered cases (KDAB-L, and KDAB-H) are presented in Tables 2 and 3. The presented results concern the maximum values of the systems main dynamic responses.

Considering the BIS system, the deck's relative displacement is observed to be prohibitively high, as expected (*mean* $u_B = 18.3$ cm), while at the same time presents a great reduction to the deck's absolute acceleration compared with the PGA. The use an alternative flexible base with the KDAB-L system, also presents very high reduction, more than 60%, of the deck's absolute accelerations, and at the same time, the base's relative displacement is 50% lower compared with the BIS (*mea* nu_B= 9.0 cm). The use of a stiffer base, with the KDAB-H system, manages to improve the structures dynamic behavior by reducing the absolute accelerations more than 25% and retain the base's relative displacement to very low levels (*mean* u_B= 3.8 cm). This makes possible the implementation of such a device, for base isolation, without conventional seismic isolation bearings.

5 Conclusions

In this paper, the KDamper is implemented for seismic protection of a bridge structure, as an alternative or supplement of conventional seismic isolation bearings. A complete analytical approach for the selection of the KDamper parameters for acceleration optimization, under base excitation, is considered. A compatible ground motion spectrum is calculated from a database of artificial accelerograms and the response power spectral densities and mean square responses are defined and verified

in the time domain. Finally, a spectral driven optimization of the KDamper parameters natural frequency is considered, and the following conclusive comments can be made:

- The optimal design of the KDamper, for an optimization of the structure's absolute acceleration transfer function, achieves an improved dynamic structural response.
- A compatible ground motion spectrum, generated from a database of artificial accelerograms, can be used to define the root mean square responses. The results confirm the ability of the root mean square responses to represent accurately the effect of the variation of the natural or base's frequency to the system responses.
- The KDamper with a nominal frequency equal to the low frequency of a conventional base isolation system (0.4 Hz), mentioned in the paper as KDAB-L, presents similar reduction to the deck's absolute accelerations with the BIS system, more than 60%, and at the same time the deck's mean maximum relative displacement is 50% than that of the BIS system ($u_{B,\,BIS}$= 18.3 cm, $u_{B,\,KDAB\text{-}L}$= 9.0 cm).
- The KDamper as a stiffer base absorption system, with a nominal frequency much higher (*1* Hz) than that of the BIS system, leads to a substantial reduction of the base's relative displacement ($u_{B,\,KDAB\text{-}H}$= 3.8 cm) combined with an acceptable structure performance with respect to the deck's absolute acceleration, with reductions more than 25%.

Acknowledgements This research has been co-financed by the European Union and Greek national funds through the Operational Program Competitiveness, Entrepreneurship, and Innovation, under the call RESEARCH—CREATE—INNOVATE (project code: T1EDK-02827).

Appendix

In the limit cases of ζ_D= 0 or$\zeta_D \to \infty$, H_{AS} of Eq. (8) becomes

$$H_{AS}(0) = \left|\frac{A}{C}\right|;\ H_{AS}(\infty) = \left|\frac{B}{D}\right| \tag{A.1}$$

The transfer function $H_{AS}(q,\zeta_D)$ of Eq. (8) has two poles for two different values of q and therefore, it presents two different maximal values (peaks) at these points. The optimal selection of the parameters of the KDamper requires that both these peaks are minimized and become equal to each other. This is ensured by the optimal

design approach followed in Den Hartog [21], which will be also used in the current paper. The approach is based on the identification of a pair of frequencies $q_L < 1$ and $q_R > 1$, where the values $H_{AS}(q_L)$ and $H_{AS}(q_R)$ become independent of ζ_D. The first step for the optimization procedure is the requirement that the values of the transfer functions at these points are equal:

$$H_{AS}(q_L) = H_{AS}(q_R) = H_{ASI} = H_{AS}(\infty) \tag{A.2}$$

In order that a solution for such a pair of frequencies exists, two alternative conditions must be fulfilled as in Den Hartog [21]:

Case I:

$$AD = BC \tag{A.3a}$$

Case II:

$$AD = -BC \tag{A.3b}$$

As it can be verified, no solution of Equation (A.3a) exists for a positive q^2, when the values $\kappa, \mu,$ and ρ are positive. Elaboration of Equation (A3.b) results to:

$$(A_2D_2 + B_0)q^4 + (A_0D_2 + A_2D_0 + B_0C_2)q^2 + (A_0D_0 + B_0C_0) = 0, \tag{A.4}$$

where

$$A = A_2q^2 + A_0;\ B = B_0\rho q;\ C = q^4 + C_2q^2 + C_0;\ D = (D_2q^2 + D_0)\rho q \tag{A.5}$$

$$A_2 = A_{2\rho}\rho^2 + A_{20};\ A_0 = A_{0\rho}\rho^2 + A_{00};\ B_0 = B_{0\rho}\rho^2 + B_{00};\ C_2 = C_{2\rho}\rho^2 + C_{20}. \tag{A.6a}$$

$$C_0 = C_{0\rho}\rho^2 + C_{00};\ D_2 = D_{2\rho}\rho^2 + D_{20};\ D_0 = D_{0\rho}\rho^2 + D_{00}. \tag{A.6b}$$

$$A_\rho = (A_{0\rho}D_{2\rho} + A_{2\rho}D_{0\rho} + B_{0\rho}C_{2\rho})D_{20} - 2(A_{2\rho}D_{20} + A_{20}D_{2\rho} + B_{0\rho})D_{0\rho}. \tag{A.7a}$$

$$B_{\rho A} = [(A_{0\rho}D_{20} + D_{2\rho}A_{00}) + (A_{2\rho}D_{00} + D_{0\rho}A_{20}) + (B_{0\rho}C_{20} + C_{2\rho}B_{00})]D_{20}. \tag{A.7b}$$

$$B_{\rho B} = -2(A_{2\rho}D_{20} + A_{20}D_{2\rho} + B_{0\rho})D_{00} - 2(A_{20}D_{20} + B_{00})D_{0\rho} \tag{A.7c}$$

$$B_\rho = B_{\rho A} + B_{\rho B}. \tag{A.7d}$$

Table A1 Coefficients in Eqs. A.6a, A.6b

	A_{2i}	A_{0i}	B_{0i}	C_{2i}	C_{0i}	D_{2i}	D_{0i}
$i = \rho$	$-\kappa(1+\kappa)\mu$	1	$\kappa^2\mu$	$-[1+(1+\kappa)^2\mu]$	1	0	$\kappa^2\mu$
$i = 0$	-1	0	1	-1	0	$-(1+\mu)$	1

$$C_\rho = (A_{00}D_{20} + A_{20}D_{00} + B_{00}C_{20})D_{20} - 2(A_{20}D_{20} + B_{00})D_{00} \tag{A.7c}$$

and the coefficients in the Eqs. (A.6a, A.6b) are defined in Table A1.

As a result of Eq. (A.4), the pair of roots of Eq. (A.4) must satisfy

$$q_L^2 + q_R^2 = -\frac{(A_0D_2 + A_2D_0 + B_0C_2)}{(A_2D_2 + B_0)}. \tag{A.8}$$

Additionally, both roots q_L and $q_R$must fulfill Eq. (A.1.b), which results in:

$$\frac{B_0}{D_0 + D_2q_L^2} = -\frac{B_0}{D_0 + D_2q_R^2} \Rightarrow q_L^2 + q_R^2 = -\frac{2D_0}{D_2}. \tag{A.9}$$

The combination of Eqs. (A.8) and (A.9) leads to an equation for the optimal value of the parameter ρ:

$$A_\rho\rho^4 + B_\rho\rho^2 + C_\rho = 0. \tag{A.10}$$

The optimal value of ρ is selected as the minimum positive value of the two roots of (A.10).

References

1. Naeim F, Kelly JM (1999) Design of seismic isolated structures: from theory to practice. Wiley, New York. https://doi.org/10.1002/9780470172742
2. Farag MMN, Mehanny SSF, Bakhoum MM (2015) Establishing optimal gap size for precast beam bridges with a buffer-gap-elastomeric bearings system. Earthq Struct 9(1):95–219. https://doi.org/10.12989/eas.2015.9.1.195
3. Molyneaux W (1957) Supports for vibration isolation. Technical report, Aeronautical Research Council, C.P. No. 322, London
4. Platus DL (1999) Negative-stiffness-mechanism vibration isolation systems. In: SPIE's international symposium on optical science engineering and instrumentation, pp 98–105. https://doi.org/10.1117/12.363841
5. Carella A, Brennan MJ, Waters TP (2007) Static analysis of a passive vibration isolator with quasi-zero-stiffness characteristic. J Sound Vib 301:678–689. https://doi.org/10.1016/j.jsv.2006.10.011
6. Ibrahim R (2008) Recent advances in nonlinear passive vibration isolators. J Sound Vib 314:371–452. https://doi.org/10.1016/j.jsv.2008.01.014

7. Nagarajaiah S, Reinhorn AM, Constantinou MC, Taylor D, Pasala DTR, Sarlis AA (2010) Adaptive negative stiffness: a new structural modification approach for seismic protection. Proceedings of the 5th WCSCM, p 103
8. Winterflood J, Blair D, Slagmolen B (2002) High performance vibration isolation using springs in Euler column buckling mode. Phys Lett A 300:122–130. https://doi.org/10.1016/s0375-9601(02)00258-x
9. Virgin LN, Santillan ST, Plaut RH (2008) Vibration isolation using extreme geometric nonlinearity. J Sound Vib 315:721–731. https://doi.org/10.1016/j.jsv.2007.12.025
10. DeSalvo R (2007) Passive nonlinear, mechanical structures for seismic attenuation. J Comp Nonlinear Dyn 2:290–298. https://doi.org/10.1115/1.2754305
11. Iemura H, Pradono MH (2009) Advances in the development of pseudo- negative-stiffness dampers for seismic response control. Struct Control Health Monit 16:784–799. https://doi.org/10.1002/stc.345
12. Attary N, Symans M, Nagarajaiah S, Reinhorn AM, Constantinou MC, Taylor D, Sarlis AA, Pasala DTR (2012) Application of negative stiffness devices for seismic protection of bridge structures. In: Proceedings of 2012 ASCE structures **congress**, Chicago. https://doi.org/10.1061/9780784412367.045
13. Attary N, Symans M, Nagarajaiah S, Reinhorn AM, Constantinou MC, Taylor D, Pasala DTR, Sarlis AA (2012) Performance evaluation of a seismically-isolated bridge structure with adaptive passive negative stiffness. In: Proceedings of 15th WCEE, Lisbon
14. Pasala DTR, Sarlis AA, Nagarajaiah S, Reinhorn AM, Constantinou MC, Taylor D (2012) Negative stiffness device for seismic protection of multistory structures. In: Proceedings of 2012 ASCE structures **congress**, Chicago
15. Sarlis AA, Pasala DTR, Constantinou MC, Reinhorn AM, Nagarajaiah S, Taylor D (2011) Negative stiffness device for seismic protection of structures—an analytical and experimental study. In: Proceedings of the 3rd COMPDYN, Corfu, Greece
16. Sarlis AA, Pasala DTR, Constantinou MC, Reinhorn A, Nagarajaiah S, Taylor D (2012) Negative stiffness device for seismic protection of structures. J Struct Eng 139:1124–1133. https://doi.org/10.1061/(asce)st.1943-541x.0000616
17. Anagnostopoulos SA, Spiliopoulos KV (1992) An investigation of earthquake induced pounding between adjacent buildings. Earthq Eng Struct Dyn 21:289–302
18. Symans MD, Charney FA, Whittaker AS, Constantinou MC, Kircher CA, Johnson MW et al (2008) Energy dissipation systems for seismic applications: current practice and recent developments. J Struct Eng 134(1):3–21. https://doi.org/10.1061/(asce)0733-9445(2008)134:1(3)
19. Kelly JM (1999) The role of damping in seismic isolation. Earthq Eng Struct Dyn 28:3–20. https://doi.org/10.1002/(sici)1096-9845(199901)28:1%3c3:aid-eqe801%3e3.0.co;2-d
20. Frahm H (1909) Device for damping vibrations of bodies. US patent #989958
21. Den Hartog JP (1956) Mechanical vibrations, 4th edn. McGraw-Hill, New York
22. Qin L, Yan W, Li Y (2009) Design of frictional pendulum TMD and its wind control effectiveness. Earthq Eng Eng Vib 29:153–157
23. McNamara RJ (1979) Tuned mass dampers for buildings. ASCE, J Struct Div 105:2766–2772
24. Luft RW (1977) Optimal tuned mass dampers for buildings. ASCE, J Struct Div 103:1985–1998
25. Haskett T, Breukelman B, Robinson J, Kottelenberg J (2003) Tuned mass dampers under excessive structural excitation. Report of the Motioneering Inc. Guelph, Ontario, Canada NIK 1B8
26. Debnath N, Deb SK, Dutta A (2015) Multi-modal vibration control of truss bridges with tuned mass dampers under general loading. J Vib Control 22(20):4121–4140. https://doi.org/10.1177/1077546315571172
27. Weber B, Feltrin G (2010) Assessment of long-term behavior of tuned mass dampers by system identification. Eng Struct 32:3670–3682. https://doi.org/10.1016/j.engstruct.2010.08.011
28. Antoniadis IA, Kanarachos SA, Gryllias K, Sapountzakis IE (2016) KDamping: a stiffness based vibration absorption concept. J Vib Control 24(3):588–606. https://doi.org/10.1177/1077546316646514

29. Antoniadis IA, Sapountzakis IE, Chatzi EF (2016) A kdamping concept for seismic excitation absorption. In: Proceedings of the 1st ICONHIC 2016, Chania, Crete, Greece, 28–30 June 2016
30. Sapountzakis EJ, Syrimi PG, Pantazis IA, Antoniadis IA (2016) KDamper concept in seismic isolation of bridges. In: Proceedings of the 1st ICONHIC 2016, Chania, Crete, Greece, 28–30 June 2016
31. Sapountzaki EJ, Syrimi PG, Pantazis IA, Antoniadis IA (2017) KDamper concept in seismic isolation of bridges with flexible piers. Eng Struct 153:525–539. https://doi.org/10.1016/j.engstruct.2017.10.044
32. Kapasakalis KA, Sapountzakis EJ, Antoniadis IA (2018) Kdamper concept in seismic isolation of building structures with soil structure interaction. In: The 13th international conference on computational structures technology (CST2018), Sitges, Barcelona, Spain, 4–6 Sept 2018
33. Syrimi PG, Sapountzakis EJ, Tsiatas GC, Antoniadis IA Parameter optimization of the KDamper concept in seismic isolation of bridges using harmony search algorithm. In: Proceedings of the 6th COMPDYN 2017, Rhodes Island, Greece, 15–17 June 2017
34. Giaralis A, Spanos PD (2012) Derivation of response spectrum compatible non-stationary stochastic processes relying on Monte Carlo-based peak factor estimation. Earthq Struct 3:581–609. https://doi.org/10.12989/eas.2012.3.3_4.581
35. Cacciola P, D'Amico L (2015) Response-spectrum-compatible ground motion processes. Encycl Earthq Eng https://doi.org/10.1007/978-3-642-36197-5_325-1
36. Seismosoft (2018) SeismoArtif–a computer program for generating artificial earthquake accelerograms matched to a specific target response spectrum. http://www.seismosoft.com
37. Saragoni GR, Hart GC (1974) Simulation of artificial earthquakes. Earthq Eng Struct Dyn 2:219–267. https://doi.org/10.1002/eqe.4290020305